JOURNAL OF CATALYSIS 13, 413–424 (1969)

Mechanisms and Kinetics of Aqueous Formic Acid and Formate Ion Dehydrogenation on Platinum and Subsequent Reaction of Adsorbed Hydrogen

SIGMUND SCHULDINER AND BERNARD J. PIERSMA*

From the Naval Research Laboratory, Washington, D. C. 20390

Received October 22, 1968; revised November 26, 1968

The open-circuit chemical behavior of dissolved HCOOH and HCOONa at Pt electrodes was studied. A double-pulse electrochemical anodic charging technique was used to first strip the surface and to then quantitatively determine the amount of atomic hydrogen formed on the clean electrode from the dissociation of formic acid and formates and the net rate at which this atomic hydrogen was removed from the electrode surface by reaction with formate species. The integrated rates of the reaction of Pt-O_{ads} with hydrogen and/or formate species, of the dehydrogenation of formic acid and formates on clean Pt, and of the atomic hydrogen removal were measured. The kinetics of the net atomic hydrogen removal process were determined and shown to be first order in respect to hydrogen atom concentration at the surface. The formation of residues from the organic free radicals which were the products of dehydrogenation retarded the further dissociation of formic acid and formates. Sulfuric acid solutions of very low pH values and molecular hydrogen could strongly affect the reaction rates and retarded the rate of hydrogen atom removal from the electrode surface. Generalizations concerning fuel cell anodic reactions are made.

The reaction of formic acid at platinum electrodes is of fundamental importance for the understanding of anodic organic reactions since this compound is the simplest organic molecule (requiring the fewest electron-transfer steps for complete oxidation) which may be usable for fuel cell technology. Although much attention has been devoted to this reaction, mechanisms in aqueous solutions have not been firmly established. The open-circuit behavior of formic acid on a Pt electrode requires elucidation; adsorption studies are incomplete, adsorbed species have not been adequately identified, and true steady-state measurements of coverage and kinetic parameters have not been reported (1). Furthermore, it is believed that control of the experimental conditions has, in general, not been adequate.

We have studied, under open-circuit conditions, the chemical behavior of dissolved HCOOH and HCOONa at Pt electrodes in the closed system developed at this laboratory (*2*). A double-pulse electrochemical anodic charging technique (*3*) is employed to obtain quantitative information on the amounts of formic acid and formate ion dehydrogenation on clean, bright Pt and on the subsequent loss of the sorbed H atoms, H_a, formed during this dehydrogenation. Concentration changes of H_a with time are used to determine the integrated rate of the dehydrogenation process and the kinetics of the net H_a removal process. It should be noted that in this paper all of the atomic hydrogen associated with the Pt surface, weakly and strongly adsorbed and dermasorbed (H atoms in the upper 2 or 3 atomic layers of Pt), is lumped together in the quantity H_a and is called sorbed atomic hydrogen.

---

* Permanent address: Eastern Baptist College, St. Davids, Pennsylvania.

EXPERIMENTAL

The closed system of glass pipe construction, the helium and hydrogen purification, and the platinum electrodes and miniature glass reference electrodes have been described previously (*2*). The general procedures for solution preparation, electrochemical cell, and solution cleaning, and preelectrolysis techniques have been reported in the same reference. The formic acid and sodium formate were of reagent grade and were used without further treatment. Ultrapure sulfuric acid (E. Merck A.G., Darmstadt) was used. The Pt bead working electrodes were 0.35 and 0.45 true cm^2 in the two systems used. These true areas were determined from the linear oxygen atom adsorption regions of anodic charging curves taken in clean, hydrogen-saturated 1.0 M H_2SO_4 solutions (*2*). For cleanliness criteria see refs. (*2*) and (*4*). Measurements were made in helium-saturated and hydrogen-saturated solutions (1 atm) of the following compositions: 1 M HCOONa, pH = 7.9; 1 M HCOONa + 1 M HCOOH, pH = 3.5; 1 M HCOOH + 1 M H_2SO_4, pH $\approx$ 0; and 0.1 M HCOOH + 1 M H_2SO_4, pH $\approx$ 0. All results were obtained at 25° ± 1°C. All potentials are reported with reference to the reversible hydrogen electrode in the same solution (RHE).

The decay time measurements (time for reduction of one monolayer of atomic oxygen by reaction with hydrogen and/or organic species in solution) were made as previously reported (*5*, *6*). A monolayer of atomic oxygen was deposited on the Pt electrode ($Pt\text{-}O_{ads}$) with a high-current-density (1–2 amp/cm^2) galvanostatic anodic pulse from an ElectroPulse, Model 3450C or Model 3450D pulse generator. The specific monolayer oxygen region was determined from longer pulses (*5*) and the proper pulse length set on the pulse generator. A Tektronix type 547 oscilloscope with type 1A1 preamplifier was used to display the data, which was then recorded on film. The solution IR drop was largely removed from the display by subtracting the appropriately attenuated rectangular pulse at the generator output from the signal across the cell (*3*).

At set times following the first pulse which oxidized the steady state adsorbed organic species on the electrode surface and deposited one monolayer of atomic oxygen, a second identical pulse was applied. A Hewlett-Packard 5214L Electronic Counter provided accurately spaced triggering pulses to the pulse generator (*3*). The time intervals (10^{-3} to 100 sec) between the two pulses were known to within 10^{-3} sec. For time intervals greater than 100 sec, the second pulse was triggered manually, with the time interval being known to about 0.1 sec.

RESULTS

A schematic diagram illustrating the double-pulse technique and showing the regions of interest is given in Fig. 1. A galvanostatic anodic pulse (1–2 amp/cm^2) was applied at the open-circuit potential (which is the reversible hydrogen potential in H_2-saturated solutions and is approximately 0.1 V in He-saturated solutions) to form one monolayer of atomic oxygen on the Pt surface. At pulse cutoff, the electrode potential decreases as the adsorbed oxygen is removed by reaction with hydrogen and/or formate species in solution. The removal of adsorbed atomic oxygen in this region has been shown previously (*3*, *4*, *6*). Typical potential-decay curves are shown in Fig. 2. The Pt surface is essentially free of adsorbed oxygen atoms, organic species, and hydrogen at the end of the $Pt\text{-}O_{ads}$ reduction region where the potential is about 0.2 to 0.3 V. This end point is the termination of a sharp fall in potential. The potential-decay region, τ_{decay}, shown in Fig. 1 is more precisely defined as the time interval after which adsorbed atomic hydrogen is first detected in the second anodic pulse. The curves in Fig. 2 are, in fact, potentiometric titrations of one monolayer of adsorbed atomic oxygen.

The minimum potentials reached after τ_{decay} (Fig. 2) varied considerably in different solutions. In HCOONa, this minimum was the initial open-circuit potential. In HCOOH + HCOONa solutions, the potential minimum was 0.05 to 0.1 V negative to the

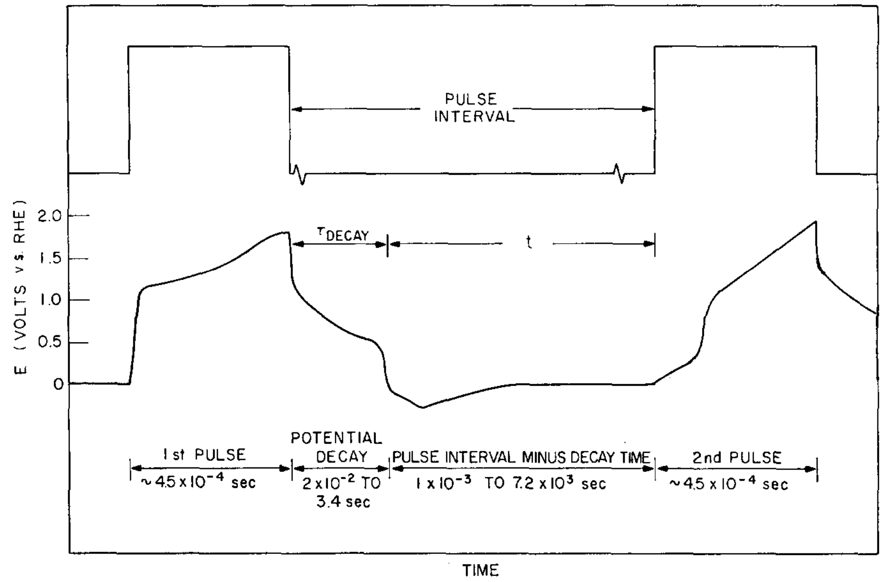

FIG. 1. Schematic diagram for the double-pulse method showing typical system response.

initial open-circuit potential and then slowly increased to that value. For HCOOH + H_2SO_4 solutions, the potential decayed to 0.35 to 0.40 V negative to the initial open-circuit potential and then rapidly increased to the open-circuit value.

An example of a typical response to a double pulse is given in Fig. 3(a). A low-potential region in which hydrogen is oxidized is not observed in the initial pulse response (top trace) but is clearly developed in the second pulse response. The progressive development of this region is well illustrated in Fig. 3(b). (In this photo, the first pulses have not been recorded.) Beginning with the bottom trace and moving upward, the amount of hydrogen present on the electrode increases as the interval between the first and second pulse is lengthened. Only the beginning portions (approximately the first third) of the anodic pulses are displayed in Fig. 3(b) to show the hydrogen regions more clearly. Similar results were obtained for He-saturated solutions.

Both the dehydrogenation reaction and the subsequent removal of hydrogen atoms by reaction with formic acid and/or formates occurred under open circuit in the pulse interval time t, Fig. 1. The second pulse was used to quantitatively determine the amount of hydrogen associated with the Pt surface at time, t.

Following τ_{decay} the hydrogen sorbed on the electrode builds up to a maximum which varied in amount and in time in the different solutions (Table 1) and was subsequently removed by reaction with formate species (the term formate species is used here to include any of the possible forms of organic species present in the HCOOH and/or HCOONa solutions which adsorb and react at the Pt surface). Figures 4 to 7 present the data from the second pulses and give the amounts [microcoulombs (μC)/cm^2] of hydrogen atom formation (corrected for double-layer charging) and of net H_a removal at given times after τ_{decay} in the different systems studied. The rate of H_a removal at open circuit after an initial period can be represented by a simple first order kinetic equation:

$$q_{H_a} = q_{0,H_a} \exp(-kt) \qquad (1)$$

where q_{H_a} is the amount of sorbed hydrogen in microcoulombs/cm^2 at any time t (defined in Fig. 1) and q_{0,H_a} is the initial amount of sorbed hydrogen determined by extrapolating (dashed lines, Figs. 4 to 7) to $t = 0$. Values of q_{0,H_a} and k obtained for the

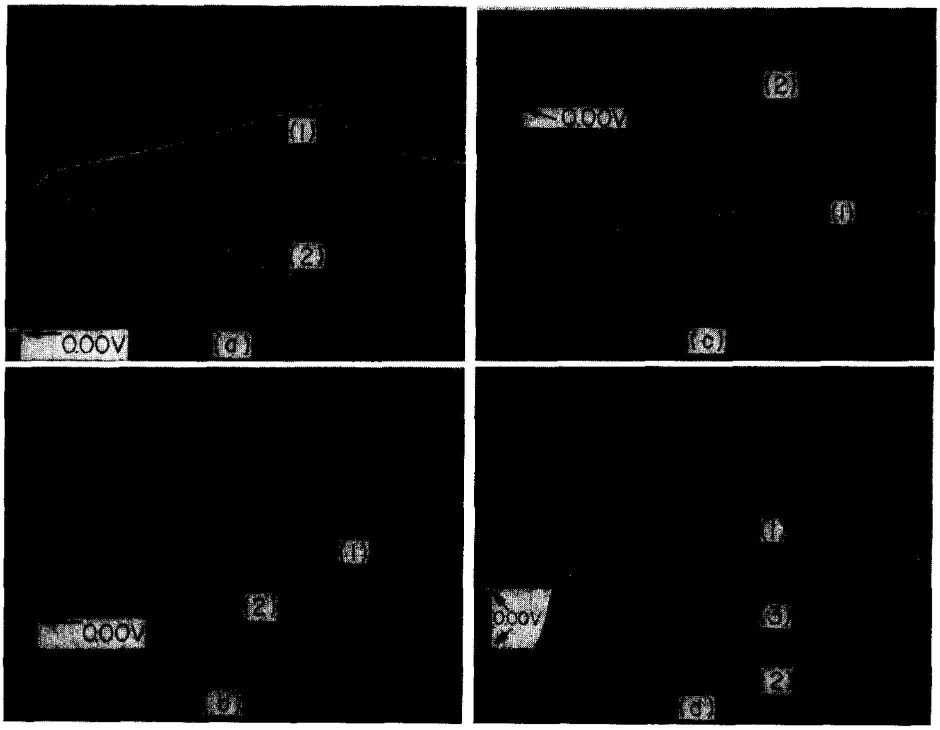

FIG. 2. Comparison of potential decay behavior in different electrolytes: (a) 1 *M* HCOONa, H_2 saturated, $i = 1.3$ amp/cm^2 (pulse amplitude). Trace 1, anodic pulse to form one monolayer of Pt-O_{ads}; abscissa 100 μsec/cm, ordinate 0.5 V/cm. Trace 2, potential decay; abscissa, 5 msec/cm, ordinate, 0.5 V/cm. (b) 1 *M* HCOOH + 1 *M* HCOONa, H_2 saturated, $i = 1.9$ amp/cm^2 (pulse amplitude). Trace 1, same as in (a). Trace 2, potential decay; abscissa, 20 msec/cm, ordinate, 0.5 V/cm. (c) 1 *M* HCOOH + 1 *M* H_2SO_4, H_2 saturated, $i = 1.9$ amp/cm^2 (pulse amplitude). Trace 1, same as in (a). Trace 2, potential decay; abscissa, 500 msec/cm, ordinate, 0.5 V/cm. (d) 0.1 *M* HCOOH + 1 *M* H_2SO_4, He saturated, $i = 1.9$ amp/cm^2 (pulse amplitude). Trace 1, same as in (a). Trace 2, potential decay; abscissa, 100 msec/cm; ordinate, 0.5 V/cm. Trace 3, potential decay; abscissa, 50 msec/cm; ordinate, 0.5 V/cm.

TABLE 1

KINETIC PARAMETERS

	Helium saturated					Hydrogen saturated				
Solution	τ_{decay} (sec)	$t_{H_a,max}$ (sec)	$q_{H_a,max}$ (μC/cm^2)	q_{O,H_a} (μC/cm^2)	k (sec^{-1})	τ_{decay} (sec)	$t_{H_a,max}$ (sec)	$q_{H_a,max}$ (μC/cm^2)	q_{O,H_a} (μC/cm^2)	k (sec^{-1})
1 *M* HCOOH + 1 *M* H_2SO_4	0.86	0.10	49	24	6.6×10^{-3}	0.26	0.20	200	120	1.1×10^{-3}
0.1 *M* HCOOH + 1 *M* H_2SO_4	3.4	0.21	49	24	2.3×10^{-3}	0.41	0.14	200	120	6.8×10^{-4}
1 *M* HCOOH + 1 *M* HCOONa	0.050	0.020	130	120	0.46	0.048	0.040	185	94	0.10
1 *M* HCOONa	0.020	0.020	150	110	8.2×10^{-2}	~0.02	0.15	360	195	2.0×10^{-2}

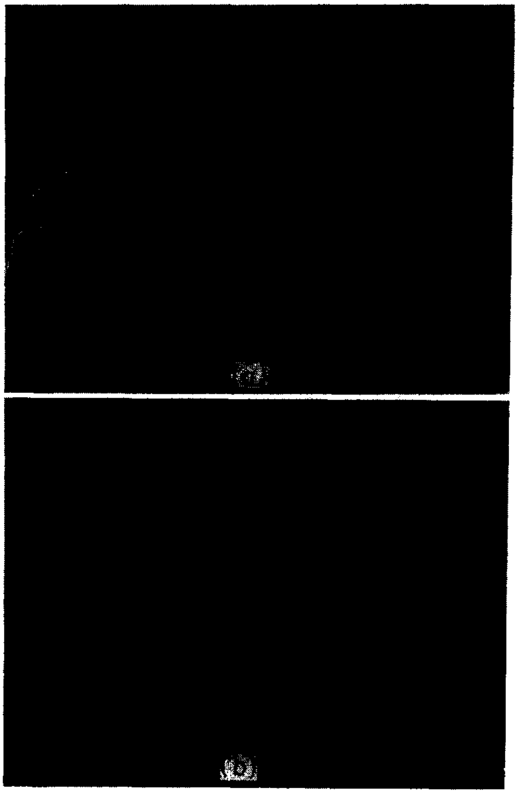

FIG. 3. (a) Typical oscilloscope traces of first (top, no hydrogen region) and second anodic galvanostatic pulses; 1 *M* HCOONa, H_2 saturated, $i = 1.3$ amp/cm^2 (pulse amplitude), 3 sec between pulses; abscissa, 50 μsec/cm; ordinate, 0.5 V/cm. (b) Series of second pulses at increasing *t* for 1 *M* HCOOH + 1 *M* H_2SO_4, H_2 saturated, $i = 1.9$ amp/cm^2 (pulse amplitude); abscissa, 20 μsec/cm. Beginning with bottom trace, *t* is (1) 0.00, (2) 0.01, (3) 0.02, (4) 0.03, (5) 0.04, (6) 0.05, and (7) 0.06 sec.

different systems examined are listed in Table 1.

Table 1 also contains values for the maximum amount of hydrogen sorbed, $q_{H_a,\max}$, and the time interval required to reach this maximum, $t_{H_a,\max}$. As can be seen in Table 1 and in Figs. 4 to 7, $q_{H_a,\max}$ is always greater than q_{0,H_a}. This condition arises because at the defined termination of τ_{decay} $(t = 0)$ the primary reaction is dehydrogenation of formate, and H_a is being deposited faster than it is being lost. However, the rate of the H_a removal reaction is faster at the actual coverages higher than q_{0,H_a} and the kinetics for the H_a removal reaction are not the same as indicated in Eq. (1). In the linear H_a removal regions of Figs. 4–7, the H_a loss from the surface is the primary process. One always should bear in mind that in all of the reaction regions described, there is an overlapping of several processes occurring at the same time at different rates. The advantage of the experimental technique used and of the subsequent analysis of the data obtained is that an adequate separation, in time, of the various regions in which a particular reaction predominates, is possible.

It is interesting that in all of these systems even though no H_a could be detected on the Pt surface upon application of the first pulse, the electrode potentials were at the open-circuit values of 0.00 V (RHE) in H_2-saturated solutions, i.e., the normal reversible hydrogen potential, and about 0.10 V in He-saturated solutions. This observation was checked very carefully in the several systems studied, and it gives

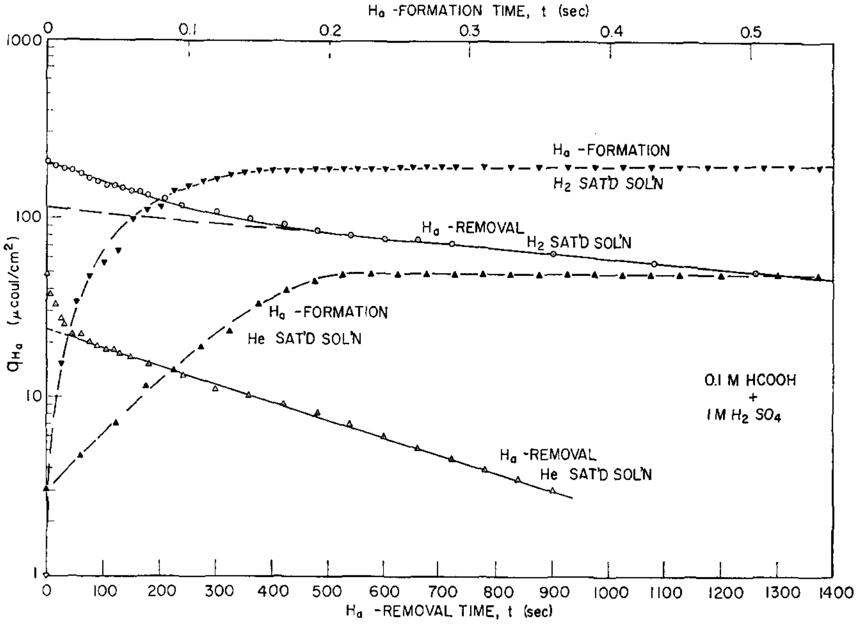

Fig. 4. Net rates of H_a formation and removal for 0.1 *M* HCOOH + 1 *M* H_2SO_4 solutions: i = 1.2 amp/cm² (pulse amplitude); ▲, H_a formation in He-saturated solution; △, H_a removal in He-saturated solution; ▼, H_a formation in H_2-saturated solution; ○, H_a removal in H_2-saturated solution.

further strong support to the view that the hydrogen equilibrium potential on Pt is controlled by extremely small amounts of weakly adsorbed atomic hydrogen in rapid exchange with hydrogen ions and with H_2 in solution (*2*, *7*, *8*).

In Fig. 6, the net H_a removal curves give an indication of the reproducibility of the

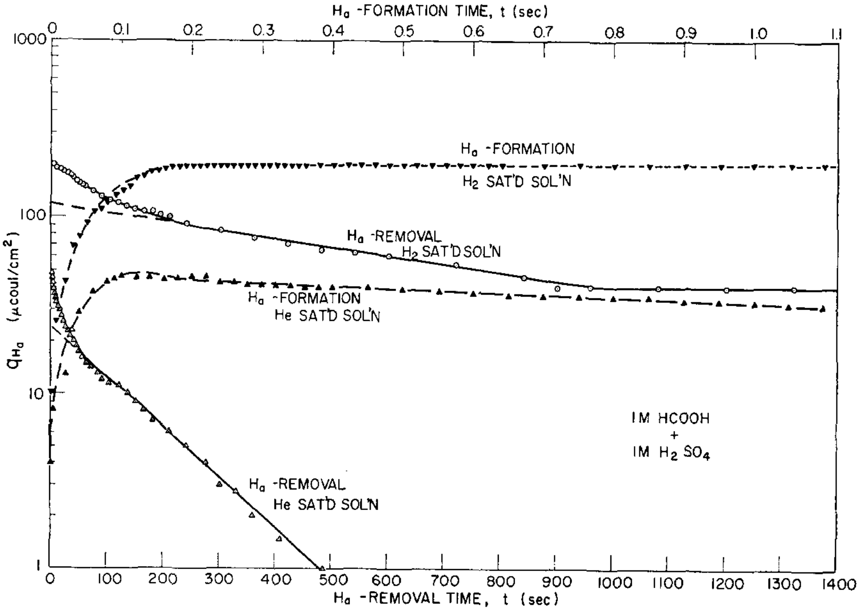

Fig. 5. Net rates of H_a formation and removal for 1 *M* HCOOH + 1 *M* H_2SO_4 solutions: i = 1.9 amp/cm² (pulse amplitude). See Fig. 4 for meaning of symbols.

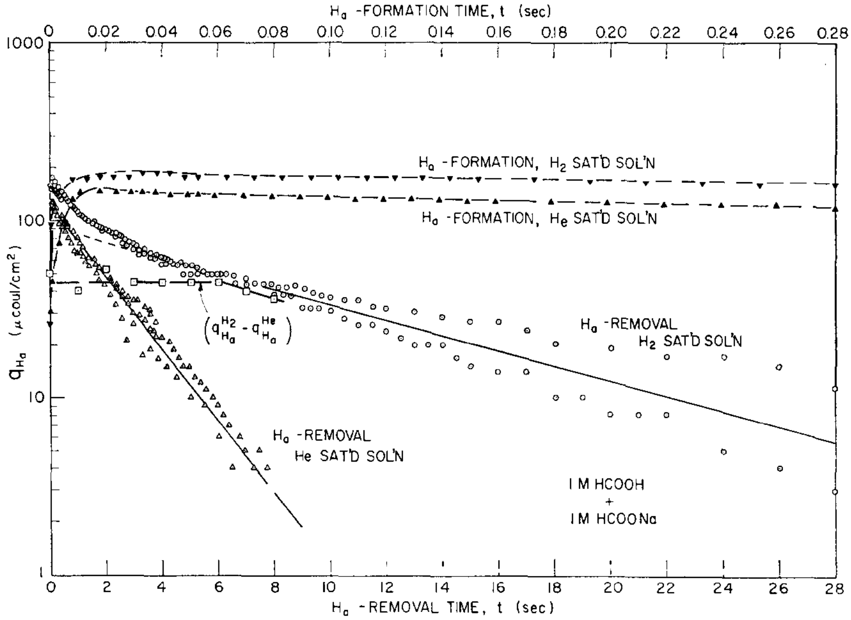

FIG. 6. Net rates of H_a formation and removal for 1 *M* HCOOH + 1 *M*HCOONa solutions: $i = 1.9$ amp/cm^2 (pulse amplitude). See Fig. 4 for meaning of symbols.

measurements. The upper and lower sets of points represent separate determinations by each of the authors in completely different systems, i.e., different solutions of the same composition, etc. The data points are shown as determined with no attempt at normalization of the results and represent rather typical differences in such determinations.

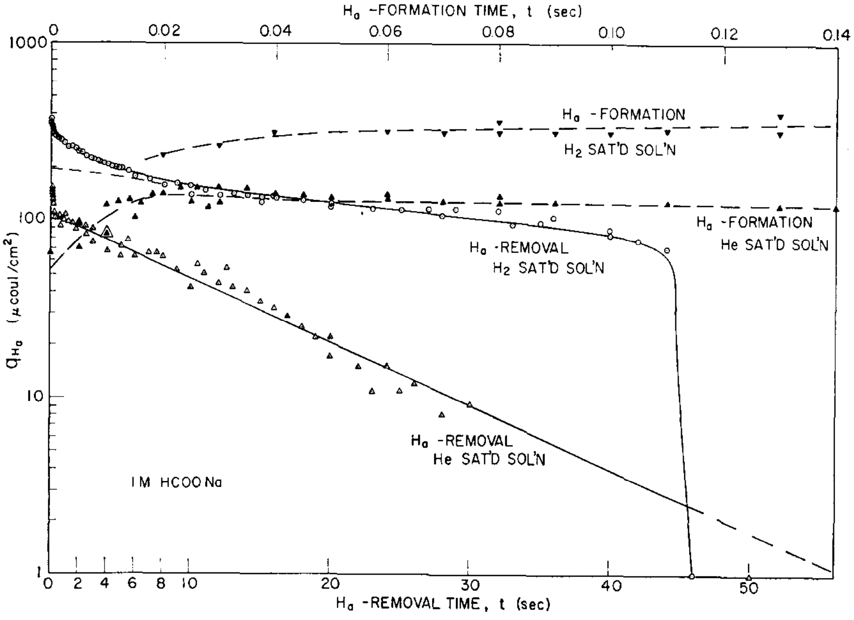

FIG. 7. Net rates of H_a formation and removal for 1 *M* HCOONa solutions: $i = 1.3$ amp/cm^2 (pulse amplitude). See Fig. 4 for meaning of symbols.

Much of the difference may be explained in the calculation of $q_{\mathrm{H_a}}$ from oscilloscopic traces since precise measurements of the length of time for each region are fairly demanding. Determinations by either author for a given system are invariably more self-consistent.

Additional data in Fig. 6, not shown in Figs. 4, 5, and 7, are for the difference between H_a determined in H_2-saturated solution, $q_{\mathrm{H_a}}^{\mathrm{H_2}}$, and H_a determined in He-saturated solution, $q_{\mathrm{H_a}}^{\mathrm{He}}$. This quantity ($q_{\mathrm{H_a}}^{\mathrm{H_2}} - q_{\mathrm{H_a}}^{\mathrm{He}}$) remains constant at about 45 μC/cm^2 until the H_a is completely removed from the Pt surface in He-saturated solution. The constancy of this quantity was not observed in any of the other systems.

DISCUSSION

The results are conveniently discussed in terms of the three basic processes encountered in formic acid–formate solutions at the Pt electrodes: (1) the removal of Pt-O_{ads} formed by the first anodic pulse by reaction with hydrogen and/or formate species, (2) the formation of H_a associated with the Pt surface, and (3) the removal of H_a and its replacement on the surface by formate species. Relative rates of these net processes are given in Table 2. In Table 2, the rates are expressed as current densities, calculated by dividing the quantity of charge associated with the adsorbed species by the time required for their complete removal or formation. These integrated rates of reaction are not absolute measures of reaction velocities and should only be used to compare the relative rates of the three processes.

1. Pt-O_{ads} Removal Region

Several studies relating specifically to this process have been reported (*9–16*). In the most thorough investigation, carried out for Pt black electrodes in 5 *N* H_2SO_4 and formic acid concentrations from 10^{-3} to 1 *M*, Oxley *et al.* (*10*) found τ_{decay} to be a function of the formic acid concentration, the oxygen coverage, and the temperature. After we extrapolated their results to a comparable basis with those reported here, we found oxygen removal rates about an order of magnitude lower than our results, e.g., about 2×10^{-5} amp/cm^2 as compared with our result of 1.2×10^{-4} amp/cm^2 for 0.1 *M* HCOOH at 25°C. Other reported values for decay times which have been obtained for solutions of approximately the same composition vary over a wide range with values of about 50 (*10*), 9 (*12*), 1000 (*14*), and 1200 to 1800 sec (*15*). The differences in oxygen coverages and amounts of dermasorbed atomic oxygen could be a primary factor for these widely scattered values [see ref. (*5*) for such oxygen effects on the rate of removal of Pt-O_{ads} with H_2].

Oxley *et al.* (*10*) suggested that two

TABLE 2

RELATIVE RATES OF NET PROCESSES

Solution	Helium saturated: Pt-O_{ads} removal (amp/cm^2)[a]	Helium saturated: H_a formation (amp/cm^2)[b]	Helium saturated: H_a removal (amp/cm^2)[b]	Hydrogen saturated: Pt-O_{ads} removal (amp/cm^2)[a]	Hydrogen saturated: H_a formation (amp/cm^2)[b]	Hydrogen saturated: H_a removal (amp/cm^2)[b]
1 *M* HCOOH + 1 *M* H_2SO_4	4.9×10^{-4}	4.9×10^{-4}	5.0×10^{-8}	1.6×10^{-3}	1.0×10^{-3}	2.8×10^{-8}
0.1 *M* HCOOH + 1 *M* H_2SO_4	1.2×10^{-4}	2.3×10^{-4}	1.7×10^{-8}	1.0×10^{-3}	1.4×10^{-3}	1.7×10^{-8}
1 *M* HCOOH + 1 *M* HCOONa	8.4×10^{-3}	6.5×10^{-3}	1.2×10^{-5}	8.8×10^{-3}	4.6×10^{-3}	2.1×10^{-6}
1 *M* HCOONa	2.1×10^{-2}	7.5×10^{-3}	1.9×10^{-6}	$\sim 2 \times 10^{-2}$	$\sim 2 \times 10^{-3}$	7.4×10^{-7}

[a] To convert to moles/cm^2 sec divide by 193 000.

[b] To convert to moles/cm^2 sec divide by 96 500.

mechanisms were responsible for the Pt-O_{ads} removal, chemical reaction above 0.9 V [Eq. (2) and an electrochemical process below 0.9 V Eqs. (3, 4)]:

$$\text{Pt-O}_{ads} + HCOOH \rightarrow CO_2 + H_2O + Pt \quad (2)$$
$$\text{Pt-O}_{ads} + 2H^+ + 2e \rightarrow Pt + H_2O \quad (3)$$
$$HCOOH \rightarrow CO_2 + 2H^+ + 2e \quad (4)$$

Breiter (*17*) from his study of Pt-O_{ads} reduction by H_2 in 1 *N* $HClO_4$ had previously reached similar conclusions, i.e., a chemical reaction, followed by an electrochemical process after bare sites became available. A detailed study of the kinetics of the Pt-O_{ads} reaction with hydrogen by Warner and Schuldiner (*3*) led to the conclusion that the rate-limiting step was the chemical reaction of Pt-O_{ads} with hydrogen at active sites. It also has been suggested (*13*), on the basis of comparisons of steady state current–potential curves with current–oxygen coverage curves taken during potential decay, that the Pt-O_{ads} removal reaction is purely electrochemical. Our results do not permit a detailed discussion of this region. We have semiquantitatively shown that the Pt-O_{ads} removal rate depends on formic acid concentration and on the oxygen coverage. Quantitative measurements of several aspects of this reaction such as carried out in refs. (*3*, *5*), e.g., the kinetics of the reaction and its dependance of τ_{decay} on Pt-O_{ads} coverage, formic acid concentration, formate ion concentration, potential, and determination of the oxygen coverage during the potential decay are necessary before a definite mechanism for this reaction can be proposed and supported.

The reaction of Pt-O_{ads} with hydrogen, formic acid, formate ions, and the effects of hydronium ions are clearly demonstrated in the lengths of the decay times (see, Table 1). It can be seen that τ_{decay} is approximately an order of magnitude greater in pH ≈ 0 formic acid solutions which contain sulfuric acid than it is in the HCOONa solutions. The decay times obtained in 1 *M* HCOONa are comparable with the shortest decay times observed in H_2 saturated 1 *M* H_2SO_4 (*6*), i.e., for the most active Pt electrodes. The contribution of H_2 to τ_{decay} (see Table 1 and the Pt-O_{ads} removal rates shown in Table 2) is very significant in the sulfuric acid solutions, but has no apparent effect on the much faster reaction in the more basic HCOONa solutions. The reason for this is due apparently to the fact that the rate of the reaction of Pt-O_{ads} with formic acid in H_2SO_4 solution is considerably slower than the rate of the reaction with hydrogen in H_2SO_4 solution. (The τ_{decay} for the Pt electrodes in pure hydrogen, 1 *M* H_2SO_4 solution was close to 0.1 sec.) Hence, in the presence of molecular hydrogen the removal of Pt-O_{ads} in HCOOH + H_2SO_4 is primarily by reaction with this hydrogen and the formic acid is inhibiting the rate of Pt-O_{ads} reduction. In the less acid formate solutions, however, the Pt-O_{ads} reaction rate with formate predominates and the influence of molecular hydrogen is small.

2. Pt-H_a Formation Region

We have observed that in the case where a potential minimum in the decay curves is reached the hydrogen atoms which are generated and sorbed on the Pt surface increase with time to a maximum. The relative rates of this reaction for the different systems studied are seen in Table 2. A comparison of these rates indicates that the formation of hydrogen atoms at low pH is faster in hydrogen than in helium-saturated solutions, but the presence of hydrogen makes less difference in the absence of sulfuric acid. Also, a much higher hydrogen coverage is reached in hydrogen-saturated solutions. Figures 4 to 7 give an accurate indication of the relative rates of atomic hydrogen formation. The rates are similar, strongly suggesting that the adsorption of formate and dissociation to H_a is as fast or faster than the same process for molecular hydrogen.

A comparison of these reactions rates also gives a good indication of the source of hydrogen, i.e., whether dissociation is from the carbon atom or from the oxygen atom of the formic acid molecule. Studies of formic acid adsorption in the gas phase have generally concluded that hydrogen dissociated from the oxygen atom. Fahrenfort *et al.* (*18*) gave strong evidence for this conclusion for the decomposition of formic acid on nickel and gold catalysts. The electrochemical literature, on the other hand, has generally assumed that dehydrogenation occurs from the carbon atom [for example, see refs. (*16*), (*19*), (*20*)]. A comparison of the rates of Pt-O_{ads} removal and H_a formation shows that these reactions occur significantly faster in solutions of higher pH where the amount of formic acid is the lowest. In other words, these reactions occur faster in solutions where the possibility of dissociation of hydrogen from the oxygen atom is minimized (HCOONa). However, one cannot conclude from this data that dehydrogenation at the OH bond does not occur.

The fact that the Pt surface is negatively charged at open circuit (*21*) does support the argument that the positive-oriented C–H end is the source of H_a rather than the negative-oriented OH end of the formic acid dipole. Similar conclusions from radiometric studies (*22*) have recently been reached for adsorbed methanol.

Since at open circuit there are no net oxidation or reduction reactions, we can write for the Pt-H_a formation reactions on the essentially clean Pt surface[*]:

$$\mathrm{HCOOH} + 2\mathrm{Pt} \rightarrow \mathrm{Pt_2\text{-}HCOOH_{ads}} \tag{5}$$

$$\mathrm{HCOO^-} + 2\mathrm{Pt} \rightarrow \mathrm{Pt_2\text{-}HCOO^-_{ads}} \tag{5a}$$

$$\mathrm{Pt_2\text{-}HCOOH_{ads}} \rightarrow \mathrm{Pt\text{-}H_a} + \mathrm{Pt\text{-}COOH_{ads}} \tag{6}$$

$$\mathrm{Pt_2\text{-}HCOO^-_{ads}} \rightarrow \mathrm{Pt\text{-}H_a} + \mathrm{Pt\text{-}COO^-_{ads}} \tag{6a}$$

$$2\mathrm{Pt} + \mathrm{H_2} \rightarrow 2\mathrm{Pt\text{-}H_a} \tag{7}$$

The H_a formation reaction requires free Pt sites since adsorbed organic species are not displaced by hydrogen. From the data in Table 2, we can write for the rate of H_a formation, $i_{H_a,f}$, in the various systems:

$$(i_{H_a,f})^{He}_{HCOONa} \approx (i_{H_a,f})^{He}_{HCOOH,HCOONa}$$
$$> (i_{H_a,f})^{H_2}_{HCOOH,HCOONa} \approx (i_{H_a,f})^{H_2}_{HCOONa}$$
$$> (i_{H_a,f})^{H_2}_{HCOOH,H_2SO_4} > (i_{H_a,f})^{He}_{HCOOH,H_2SO_4}$$

The relative rates of reactions (5) and (5a) and (6) and (6a) are greater than reaction (7) at high pH, but lower in H_2SO_4. Since the buildup of adsorbed formic acid or formate ion in the H_a formation period is not noticeable in the second pulse Pt-O_{ads} formation region, it appears that the dehydrogenation reactions (6) and (6a) are faster than reactions (5) and (5a). Otherwise one would expect a much faster buildup of organic species on the Pt surface. In addition

$$i_{H_a,f} \propto 1/[H_3O^+]$$
$$i_{H_a,f} \propto [\text{H–C–}]$$

where $[H_3O^+]$ and [H–C–] are the concentrations of hydronium ions and H–C– bonds, respectively.

Comparing H_a formation rates in 1 *M* HCOOH + 1 *M* HCOONa with 1 *M* HCOONa (Table 2) one can conclude that $[H_3O^+]$ appears to effectively cancel the effects of [H–C–] in He-saturated solution. However, in the presence of H_2, even though the Table does show twice the H_2 formation rates for the HCOOH + HCOONa solution as compared to the values determined for HCOONa solution, a generalization of the meaning of the difference in H_a formation for these two solutions is not justified because the potential decay in HCOONa solution was too diffuse (see Fig. 7) to permit an accurate determination of τ_{decay} for $t < 0.02$ sec.

The major conclusion which can be made concerning the H_a formation reaction on clean Pt is that in high pH solution, formate ion can supply atomic hydrogen faster than molecular hydrogen can. The limiting current density for molecular hydrogen dissociation is 2×10^{-3} amp/cm^2 in 1 atm H_2-saturated solution (*23*), whereas in 1 *M* HCOONa solution, the integrated rate of H_a formation in helium-saturated solution is three to four times higher (Table 2). As Tables 1 and 2 further show, the net amount of H_a formed is appreciably higher in H_2-saturated solutions than in He-saturated solution.

3. Pt-H_a Removal Region

More complete kinetic data were obtained for the much slower H_a removal reaction. The literature indicates two feasible mechanisms for the removal of H_a. The first mechanism, as given by Fahrenfort *et al.* (*18*), is possible in formic acid solutions:

---

[*] Pt-H_a, as defined in this paper, includes adsorbed and dermasorbed H atoms. Hence, net H_a quantities of over half a monolayer are possible, as were found in several cases (see Table 1).

$$H_a + HCOOH \rightarrow (OOCH)_{ads} + H_2 \qquad (8)$$

The second mechanism, given by Minakshisandaran *et al.* (*20*), is possible both in acid and alkaline solutions:

$$H_a + HCOOH \rightarrow (COOH)_{ads} + H_2 \qquad (9)$$

or,

$$H_a + HCOO^- \rightarrow (COO^-)_{ads} + H_2 \qquad (9a)$$

Although mechanisms (8) or (9) are both possible, interactions of the formate free radicals with the Pt surface and with other species at the surface, dimerization, polymerization, and other reactions must be considered as well.

The kinetics of the net H_a removal (Figs. 4 to 7) were determined [Eq. (1)] and were shown to be first order in H_a concentration. Kinetic parameters are given in Table 1. Table 2 interprets these parameters in terms of the integrated H_a removal rates. Referring to Table 2, it is obvious that the current density for the net integrated H_a removal, $i_{H_a,r}$, is related as follows:

$$[i_{H_a,r}]^{He}_{HCOOH,H_2SO_4} \approx [i_{H_a,r}]^{H_2}_{HCOOH,H_2SO_4} \ll [i_{H_a,r}]^{H_2}_{HCOONa} < [i_{H_a,r}]^{H_2}_{HCOOH,HCOONa} \approx [i_{H_a,r}]^{He}_{HCOONa} < [i_{H_a,r}]^{He}_{HCOOH,HCOONa}$$

The sulfate ion would not be adsorbed on the negatively charged Pt surface at the open-circuit potentials found during H_a removal and therefore could not account for the much lower rates in $H_2SO_4 +$ HCOOH solutions. However, formate ion, which is not symetrical, is a dipole whose positive end (H–C–) could be adsorbed on the negatively charged Pt.

It appears that in the higher pH He-saturated solutions the H_a removal is faster when HCOOH is present, i.e., reaction (8) or (9) is faster than (9a). The much slower rates of H_a loss in pH ≈ 0 and in H_2-saturated solution is most likely related to the significant reformation of H_a during the net H_a removal period.

During H_a removal hydronium ions may be reduced with an accompanying equivalent oxidation of adsorbed free radicals (8,9,9a) to CO_2 and/or CO_2 and H_a. Such a mechanism would account for the much longer times required to remove H_a in sulfuric acid solutions. Indeed, it is possible that H_2 could have similarily retarded the net removal of H_a by a simultaneous replenishment of H_a from the reduction of H_3O^+ and the oxidation of H_2 to $H_a + H^+$. The data in Fig. 5, especially, show a region where the loss of H_a in H_2-saturated solution was very slow and virtually independent of time. In addition, the organic free radical reactions to form residues which block the formation of H_a may be strongly influenced by the presence of hydronium ions.

The complexity of processes occurring during H_a removal do not allow a quantitative evaluation of the various reactions from our data. Further studies in which the effects of potential, pH, anions, concentration, identification of adsorbed organic species, etc., are necessary in order to more fully understand the variety of processes occurring. This information could be useful in maintaining a fast organic dehydrogenation process on an electrode surface over long periods of time. This appears to be a necessary condition for the successful use of organic materials for low-temperature, aqueous fuel cell operation.

CONCLUSIONS

In terms of applicability to low-temperature, aqueous fuel cell anodic reactions, several important generalizations are possible concerning fuels on suitable catalytic electrode materials.

(1) Atomic hydrogen is an excellent, and quite possibly the ideal, fuel for operation of a fuel cell anode at low polarization.

(2) On clean electrode surfaces, formic acid and formates, and possibly other organic fuels, can supply atomic hydrogen at rates comparable to, or even faster than molecular hydrogen can.

(3) The retardation of the dissociation of formates and other organic fuels to atomic hydrogen and free radicals is due to the adsorption of residues which most likely are reaction products caused by the interaction of the free radicals with the electrode surface and with each other. The very act of dehydrogenation results in a reactive bond being made available for further reaction.

(4) Sulfuric acid, and most likely other acids, and molecular hydrogen appear to retard the formation of residues on the electrode surface which hinder the dehydrogenation reaction. Higher concentrations of H_a are possible in the presence of molecular hydrogen.

(5) A slowing down of activity of catalysts for hydrogen fuel cell anodic reactions may well be largely related to the formation of similar residues due to the reaction of organic impurities.

ACKNOWLEDGMENTS

The authors are indebted to Professor P. H. Emmett, Johns Hopkins University and to Dr. Murray Rosen, Naval Research Laboratory for very helpful comments and suggestions.

REFERENCES

1. PIERSMA, B. J., AND GILEADI, E., The mechanism of oxidation of organic fuels, *in* "Modern Aspects of Electrochemistry" (J. O'M. Bockris, ed.), Vol. 4, pp. 85–87, 102–114. Plenum Press, New York, 1966.

2. SCHULDINER, S., AND ROE, R. M., *J. Electrochem. Soc.* **110**, 332, 1142 (1963).

3. WARNER, T. B., AND SCHULDINER, S., *J. Electrochem. Soc.* **115**, 28 (1968).

4. SCHULDINER, S., AND WARNER, T. B., *J. Phys. Chem.* **68**, 1223 (1964).

5. SCHULDINER, S., AND WARNER, T. B., *J. Electrochem. Soc.* **112**, 212 (1965).

6. WARNER, T. B., SCHULDINER, S., AND PIERSMA, B. J., *J. Electrochem. Soc.* **114**, 1120 (1967).

7. SCHULDINER, S., *J. Electrochem. Soc.* **106**, 891 (1959); **107**, 452 (1960); **108**, 602 (1961).

8. PRESBREY, C. H., JR., AND SCHULDINER, S., *J. Electrochem. Soc.* **108**, 985 (1961).

9. SLOTT, R., Ph.D. Thesis, Massachusetts Institute of Technology, 1963.

10. OXLEY, J. E., JOHNSON, G. K., AND BUZALSKI, B. T., *Electrochim. Acta* **9**, 897 (1964).

11. MUNSEN, R. A., *J. Electrochem. Soc.* **111**, 372 (1964).

12. GOTTLIEB, M. H., *J. Electrochem. Soc.* **111**, 465 (1964).

13. HOFFMAN, A., AND KUHN, A. T., *Electrochim. Acta* **9**, 835 (1964).

14. BREITER, M. W., *J. Electroanal. Chem.* **15**, 221 (1967).

15. ECKERT, J., *Electrochim. Acta* **12**, 307 (1967).

16. PODLOVCHENKO, B. I., PETRY, O. A., FRUMKIN, A. N., AND LAL, HIRA, *J. Electroanal. Chem.* **11**, 12 (1966).

17. BREITER, M. W., *J. Electrochem. Soc.* **109**, 425 (1962).

18. FAHRENFORT, J., VANREYEN, L. L., AND SACHTLER, W. M. H., The decomposition of formic acid on metal catalysts, *in* "The Mechanism of Heterogenous Catalysis" (J. H. deBoer, ed.), pp. 23–48. Elsevier, Amsterdam, 1960.

19. BAGOTZKY, V. S., AND VASSILIEV, YU. B., *Electrochim. Acta* **11**, 1439 (1966).

20. MINAKSHISANDARAM, N., VASSILIEV, YU. B., AND BAGOTZKY, V. S., *Elektrokhimiya* **3**, 193, 283 (1967).

21. KAZARINOV, V. E., AND BALASHOVA, N. A., *Doklady Akad. Nauk SSSR* **157**, 1174 (1964).

22. SMITH, R. E., URBACH, H. B., AND HATFIELD, N. L., *J. Phys. Chem.* **71**, 4121 (1967).

23. SCHULDINER, S., *J. Electrochem. Soc.* **115**, 362 (1968).